

Ionization probability of the hydrogen atom suddenly released from confinement

Morcillo M F, Alcaraz-Pelegrina J M, Sarsa A *

October 13, 2017

Abstract

The problem of the stability of a confined atom when it is extracted from the confining cavity has been investigated, modeled by a spherical hard wall potential. The ionization probability when the atom is released from confinement has been obtained. The dependence of the ionization probability on the confinement radius and on the quantum numbers of the initial confined state has been studied. The probability density function of the ionization energy of the ejected electron has been obtained for the different cases considered. The oscillatory structure of this distribution function, with a principal maximum located in the neighborhood of the energy of the initial state and minima very close to zero has been elucidated. The sudden approximation has been applied and the analytic continuation method has been used to calculate the different stationary states.

Keywords

confined atoms, ionization probability, ionization energy distribution function, sudden approximation.

*Departamento de Física, Campus de Rabanales Edif. C2, Universidad de Córdoba, E-14071 Córdoba, Spain email: fa1sarua@uco.es

INTRODUCTION

The development of experimental techniques for the encapsulation of atoms and molecules within carbon nanostructures¹⁻⁵ has motivated a lot of interest in the study of confined systems. Complexes with atoms or molecules trapped inside molecular cages can be employed for the storage or transport of atoms or molecules that can be used as energy sources⁶ or substances for biomedical applications⁷. Properties such as the ionization potential, atomic size, level structure, chemical reactivity or oscillator strengths, are substantially modified when the atom or molecule is spatially confined, see e.g.⁸⁻¹². These effects have been applied in fields such as optics or electronics¹³⁻¹⁵. Quantum dots are confined systems with conductivity and optical properties governed by their level structure that can be tuned by modifying the size of the confinement¹⁶. Spatial confinement can be used to model the effect of a plasma environment on properties of atoms and ions that are important for the analysis of astrophysical data and in plasma spectroscopy and diagnosis, see¹⁷ and references therein.

From a theoretical point of view, the properties of confined atoms and molecules have been studied starting from different models of confinement. A spherical hard wall with the atom in the center has been widely employed to analyze the changes in the electronic structure of the system¹⁸⁻²⁴. Finite size potentials have also been considered to study confinement by surfaces that can be penetrated by the electron charge²⁵⁻²⁸. The impenetrable spherical cavity model has shown to be a good starting point for reproducing the effects of pressure on atoms, which has proved useful for studying different confined quantum systems see e.g.²⁹, and references therein. Pressure is one of the parameters responsible for the changes in the electronic structure when atoms are embedded in solid or liquid host matrices and reversible insertion of atoms into solids is driven by a radial mechanism³⁰.

One important issue for the application of encapsulation techniques, is the possibility of storing the guest species in a reversible way. Within this context, the compressibility of atoms has been investigated in terms of the changes in volume and energy induced by the pressure exerted by the cavity³⁰. Here we board a different aspect of the problem of the encapsulation reversibility. We pose the question of the stability of the atom if it is suddenly released from the cavity. We study the time evolution of the encapsulated atom when it

emerges from the nanocavity. The pressure exerted by the environment causes the atom not to be in a steady state as it leaves the cavity. We obtain the ionization probability and the probability density function of the ionization energy for different initial states and confinement regimes. We consider ideal conditions for extraction assuming that the time needed to remove confinement can be neglected. This assumption allows us to obtain exact solutions that can be adapted to match more realistic situations and their properties define what region of parameters should be explored¹⁰. The sudden approximation, see e.g.³¹ is employed to solve the time dependent Schrödinger equation. It is worth mentioning here a similar theoretical treatment of the stability of the electronic bound states in an atom following beta decay³²

METHODOLOGY

We start from the hydrogen atom confined by a impenetrable spherical surface. We assume that initially the confined atom is in a particular stationary state

$$\Psi(\vec{r}, t) = e^{-iE_{nl}^c t/\hbar} \Psi_{nlm}^c(\vec{r}), \quad t \leq 0 \quad (1)$$

where

$$H^c \Psi_{nlm}^c(\vec{r}) = E_{nl}^c \Psi_{nlm}^c(\vec{r}) \quad (2)$$

with

$$H^c = -\frac{\hbar^2}{2m_e} \nabla^2 - \frac{Z\alpha\hbar c}{r} + v_c(r) \quad (3)$$

where m_e is the electron mass, Z the nuclear charge, α the fine structure constant and $v_c(r)$ the confining potential

$$v_c(r) = \begin{cases} 0 & \text{if } r < r_c \\ \infty & \text{if } r \geq r_c \end{cases} \quad (4)$$

Due to the spherical symmetry of the confinement, the stationary states of the confined hydrogen atom can be written in the same manner as for the free atom

$$\Psi_{nlm}^c(\vec{r}) = R_{nl}^c(r) Y_{lm}(\Omega) \quad (5)$$

with $Y_{lm}(\Omega)$ the spherical harmonics and $R_{nl}^c(r)$ can be written in terms of the radial $u_{nl}^c(r)$ function

$$u_{nl}^c(r) = r R_{nl}^c(r) \quad (6)$$

obtained as the solution of the radial Schrödinger equation

$$\frac{d^2 u}{dr^2} + \left[\epsilon_{nl}^c + \frac{\zeta}{r} - \frac{l(l+1)}{r^2} \right] u = 0 \quad (7)$$

where

$$\epsilon_{nl}^c = \frac{2m_e}{\hbar^2} E_{nl}^c, \quad \zeta = \frac{2Z\alpha m_e c}{\hbar} \quad (8)$$

The difference with the free atom is that the Dirichlet boundary condition is imposed in Equation 7

$$u(r_c) = 0 \quad (9)$$

When confinement is removed the state of the hydrogen atom can be expanded in terms of the eigenfunctions of the free atom Hamiltonian

$$\Psi^f(\vec{r}, t) = \sum_{n'=1}^{\infty} e^{-i E_{n'} t / \hbar} \sum_{l'=0}^{n'-1} \sum_{m'=-l'}^{l'} C_{n'l'm'}^{nlm} \Psi_{n'l'm'}^f(\vec{r}) + \int_0^{\infty} dE' e^{-i E' t / \hbar} \sum_{l'=0}^{\infty} \sum_{m'=-l'}^{l'} C_{l'm'}^{nlm}(E') \Psi_{E'l'm'}^f(\vec{r}) \quad (10)$$

where (n, l, m) are the quantum numbers of the initial confined state and $\Psi_{n'l'm'}^f(\vec{r})$ and $\Psi_{E'l'm'}^f(\vec{r})$ are the stationary states of the bound and continuous spectrum of the unconfined hydrogen atom respectively.

In order to use the expansion of Equation 10, the radial wave functions of the continuous spectrum must be normalized in the energy scale³³

$$\int_0^{\infty} dr u_{El}^f(r) u_{E'l}^f(r) = \delta(E - E') \quad (11)$$

where the radial $u(r)$ functions for the states of the free atom are defined as in Equations 5 and 6. The eigenfunctions of the discrete spectrum satisfy the usual normalization condition.

In our model we assume that the time needed to eliminate the confinement is short as compared with the time involved in the dynamics of the system. Then the sudden approximation can be invoked and the expansion of Equation 10 can be continued to $t = 0$, the

time when confinement is removed. The continuity condition on the wave function gives

$$\begin{aligned} C_{n'l'm'}^{mlm} &= \langle \Psi_{n'l'm'}^f | \Psi_{nlm}^c \rangle \\ &= C_{n'}^{ml} \delta_{ll'} \delta_{mm'} \end{aligned} \quad (12)$$

$$\begin{aligned} C_{l'm'}^{mlm}(E') &= \langle \Psi_{E'l'm'}^f | \Psi_{nlm}^c \rangle \\ &= C^{ml}(E') \delta_{ll'} \delta_{mm'} \end{aligned} \quad (13)$$

where

$$C_{n'}^{ml} = \int_0^\infty dr u_{n'l}^f(r) u_{nl}^c(r) \quad (14)$$

$$C^{ml}(E') = \int_0^\infty dr u_{E'l}^f(r) u_{nl}^c(r) \quad (15)$$

Note that when confinement is removed, the orbital angular momentum, l , and the magnetic number, m , do not change due to the spherical symmetry of the confining potential.

The normalization of the quantum state leads to the following sum rule

$$1 = \sum_{n'=1}^{\infty} |C_{n'}^{ml}|^2 + \int_0^\infty dE' |C^{ml}(E')|^2 \quad (16)$$

Therefore, when the confined atom is in a stationary state, $\Psi_{nlm}^c(\vec{r})$, and the confinement is suddenly removed, $|C_{n'}^{ml}|^2$ is the probability of finding the electron in the bound state $\Psi_{n'lm}^f(\vec{r})$ of the unconfined hydrogen atom. The probability, P_B , that the atom remains in a bound state is

$$P_B = \sum_{n'=1}^{\infty} |C_{n'}^{ml}|^2 \quad (17)$$

The ionization probability, P_I is

$$P_I = 1 - P_B = \int_0^\infty dE' |C^{ml}(E')|^2 \quad (18)$$

and $|C^{ml}(E')|^2 dE'$ is the probability to observe an ionized electron in the energy interval between E' and $E' + dE'$. The distribution

$$\rho_I(E') = |C^{ml}(E')|^2 \quad (19)$$

as a function of E' is the probability density function of the ionization energy.

The energy of the atom after confinement is removed can be obtained as the expectation value of the Hamiltonian of the free hydrogen atom in the final time dependent wave function of Equation 10

$$\begin{aligned} E^f &= \int d\vec{r} \Psi^f(\vec{r}, t)^* H \Psi^f(\vec{r}, t) \\ &= \int d\vec{r} \Psi_{nlm}^c(\vec{r})^* H \Psi_{nlm}^c(\vec{r}) \end{aligned} \quad (20)$$

where H is the free hydrogen atom Hamiltonian. The final state, $\Psi^f(\vec{r}, t)$, is time dependent, Equation 10, but the expectation value of the Hamiltonian is constant when confinement is removed. In the second step we have taken, $t = 0$, in the final state and we have used that within the sudden approximation the wave function does not change when confinement is removed. As the confined wave functions vanish for $r > r_c$ and within the confinement region $H = H^c$ we obtain that

$$E^f = E_{nl}^c \quad (21)$$

the energy is conserved in the sense that the expectation value of the free hydrogen atom Hamiltonian in the final state is equal to the energy eigenvalue corresponding to the initial confined state.

The radial eigenfunctions of the discrete, $u_{n'l'}^f(r)$ and continuous spectrum, $u_{E'l'}^f(r)$ are very well known, see e.g.³³. The analytic continuation method³⁴⁻³⁶ has been employed to obtain the eigenvalues and radial functions of the confined states, Equations 7 and 9. The analytic continuation method has also been used to calculate the radial functions of the continuous spectrum of the free atom with the energy scale normalization, Equation 11. In this method, the solution of the differential equation is approximated in the neighborhood of the origin by a truncated Frobenius series. Then different truncated Taylor series around the tabular points r_1, r_2, \dots are constructed. The radial function is written as a piecewise polynomial function

$$u(r) = \begin{cases} r^{l+1} \sum_{i=0}^N a_i r^i & 0 \leq r \leq r_1 \\ \sum_{i=0}^N c_{ki} (r - r_k)^i & r_k \leq r \leq r_{k+1}, \quad k = 1, 2, \dots \end{cases} \quad (22)$$

The a_i and c_{ki} coefficients are calculated in the usual way by substituting Equation 22 into Equation 7. The regularity of the radial function and the normalization condition are

employed to start the series. The values of the radial function and its first derivative at r_i , $i = 1, 2, \dots$ are obtained from the series at r_{i-1} . More details can be found in³⁴. For the bound states, the analytic continuation method is used to carry out the inward and outward integrations and the condition of the log derivative at an intermediate point is imposed to get the eigenvalue. Here we have used equally spaced tabular points with step size $\sim 10^{-4}$ Å and polynomial expansion of degree $N = 20$. With these parameters we reproduce at least 18 decimal digits of the energy eigenvalues of the highly accurate solutions of the confined hydrogen atom²¹. The integrals involved in the calculation of the amplitude probabilities $C_{n'}^{ml}$ and $C^{ml}(E')$, Equations 14 and 15, can be computed analytically starting from Equation 22.

RESULTS AND DISCUSSION

In Table 1 we provide the ionization probability after leaving confinement for different confined bound states for $r_c = 0.5292$ Å and $r_c = 1.0584$ Å. The ionization probability is calculated from Equation 18. The sum rule of Equation 16 is verified with four decimal digits. The same is reported in Table 2 to Table 5 from $r_c = 1.5875$ Å to $r_c = 5.2918$ Å. These values lie within the range of confinement radii employed by other authors in the study of confinement effects on the electronic structure of atoms. The reason is twofold, first for these values confinement effects become apparent and second these are the typical sizes of some confinement cavities, for example the value of the inner radius of C₆₀ and the pore radius of faujasite is about 3.5 Å.

As is well known, confinement removes the degeneracy in l within a given atomic shell of the hydrogen atom. The energy decreases as l increases within a shell. The ionization probability does not increase with the energy of the confined state as, in principle it could be expected.

In order to study the dependence of these results on the atomic state and the confinement radius, in Figure 1 we plot the ionization probability for states with the same orbital angular momentum, l , and different n value as a function of the r_c . These figures show how the ionization probability decreases as the confinement radius increases. The ionization probability

increases with the atomic shell, n , for those orbitals with the same orbital angular momentum, l . This behavior could be expected by taking into account that the spatial extension of the orbitals of the free hydrogen atom increases with n for fixed l values. For example, the expectation value of the radial coordinate is given by

$$\langle r \rangle_{nl} = \frac{1}{2}[3n^2 - l(l+1)]a_0 \quad (23)$$

with a_0 the Bohr radius. As confinement effects are more important for those orbitals with larger spatial extension, the ionization probability increases as n does. This is also the case for the energy of the confined orbitals.

In Figure 2 we plot the ionization probability for all of the states of the same atomic shell, i.e. orbitals with the same n and different l values. Here the behavior of the ionization probability with n and l is different for small and large values of the confinement radius. For values of r_c similar or greater than the mean radius of the free orbital, our results show that the larger the l value, the smaller the ionization probability. This is consistent with the idea that the ionization probability increases with the spatial extension of orbitals, that decreases with l for orbitals of the same atomic shell, Equation 23. Let us note that in the limit of large confinement radius, r_c , the ionization probability vanishes for all of the orbitals.

For small confinement radii as compared with $\langle r \rangle_{nl}$ the trend is the opposite, for fixed n , the ionization probability increases with l . This leads to orbitals of the same shell with higher energies and lower ionization probabilities as for example $3s$, $3p$ and $3d$ for $r_c = 1.0584$ Å. The reason for this lies in the centrifugal barrier. The r^{l+1} behavior for small electron-nucleus distances leads to radial functions for the free atom that take very small values within the confinement region. Then the overlap between confined and unconfined bound states, Equation 14, is very small.

In Figure 3 we plot the probability density function of the ionization energy, Equation 19, for different orbitals and confinement radii. The probability density functions for the ionization energy present an oscillatory structure of successive maxima and minima. As the minima are very close to zero, practically no electrons with those ionization energies could be detected. The absolute maximum is much larger than the other maxima. For confined states of negative energy the absolute maximum is located at $E = 0$, while for confined

states of positive energy the absolute maximum lies in the neighborhood of the energy of the confined state.

In order to elucidate this behavior of the probability density function for the ionization energy, we compare the radial function of the initial confined state with those of several final states of the continuous spectrum. We show here results for a confined $4s$ orbital at $r_c = 2.1167 \text{ \AA}$ which is representative of the rest of cases. In Figure 4 we plot the radial $u(r)$ function of the confined orbital as compared with radial functions of states of the continuous spectrum at different ionization energies. We also plot the product of the confined bound and free ionized radial functions that governs the probability, see Equation 15. We have considered $E = 101.7 \text{ eV}$ and $E = 181.4 \text{ eV}$ to illustrate the behavior at the absolute maximum and one minimum respectively and two intermediate values of the energy of the ionized electron, $E = 131.90$ and 156.7 eV .

For ionization energies close to the energy of the confined state, the radial functions of the initial and final states are very similar. The product of both functions is positive providing large values for $|C_{nl}(E)|^2$, see Equation 15. As E is increased, the maxima and minima of the continuous state are shifted through smaller r values, and the product of the radial functions presents positive and negative values that cancel out in the integral, see Figure 4 for $E = 131.90$ and 156.7 eV . At minima the weight of the positive and negative regions is very similar. The same will hold for energies smaller than the energy of the confined state, the nodes, maxima and minima of the radial function of the ionized state are shifted to larger r values, and the effect on $|C_{nl}(E)|^2$ is the same. We find a pattern of constructive and destructive interferences among the wave function of the initial state and the continuous wave functions of the free states at different ionization energies. This scheme is repeated for all of the ionization energies providing the structure of the probability density function.

CONCLUSIONS

The stability of a confined hydrogen atom when it is released from confinement has been studied. It has been assumed that the time needed to extract the atom is short. A spherical hard wall model has been employed for the confining potential. The ionization probability

and the probability density function of the ionization energy for different initial states and confinement radii have been obtained. A non negligible ionization probability has been obtained for some confined states of negative energy. In general the ionization probability increases with the energy of the confined state but a non-monotonic behavior has been found for some states and confinement radii. The ionization probability increases with n , the principal quantum number of the initial state. For a given state, the ionization probability is reduced as the confinement radius increases. Except for initial states of the K and L shell, the ionization probability is very important for all the confinement radii here considered. For initial states within a given shell, the ionization probability decreases with l , the orbital angular momentum quantum number for the intermediate and large confinement radii here considered. The opposite holds in the strong confinement regime. The probability density function of the ionization energy presents a structure of maxima and minima. In all of the cases studied, the global maximum is much larger than the other maxima and it lies at an energy close to the energy of the initial state when it is positive. The minima are very close to zero. This structure of the probability density function has been explained in terms of the overlap between the initial and final radial functions. Within the confinement volume, the confined radial function presents a very similar structure to the radial function of the ionized electron. In the case of the minima, the product of both radial functions presents positive and negative values that practically cancel each other.

ACKNOWLEDGMENTS

AS and JM A-P acknowledge partial support by the Spanish Dirección General de Investigación Científica y Técnica (DGICYT) and FEDER under contract FIS2015-69941-C2-2-P and by the Junta de Andalucía grant FQM378. MFM acknowledges a grant under the program "Universidad de Córdoba. II Becas Semillero de Investigación". We thank Profs. Enrique Buendía and José I. Fernández-Palop for their insightful comments during the realization of this work.

References

1. C. Liu, Y. Y. Fan, M. Liu, H. T. Cong, H. M. Cheng, M. S. Dresselhaus, *Science* **1999**, 286, 1127.
2. K. Komatsu, M. Murata, Y. Murata, *Science* **2005**, 307, 238.
3. A. J. Horsewill *et al.* *Phys. Rev. Lett.* **2009**, 102, 013001.
4. K. Kurotobi, Y. Murata, *Science* **2011**, 333, 613.
5. A. Krachmalnicoff *et al.* *Nat. Chem.* **2016**, 8, 953.
6. K. Ayub, *Int. J. Hydrogen Energy* **2017**, 42, 11439.
7. T. Li, H.C. Dorn, *Small* **2017**, 13, 1603152.
8. W. Jaskolski, *Phys. Rep.* **1996**, 271, 1.
9. J. Sabin, E. Brändas, S. Cruz (Eds.), *Theory of Confined Quantum Systems*, Vol. 57 and 58, Elsevier, San Diego **2009**.
10. J.-P. Connerade, *J. Phys.: Conf. Ser.* **2013**, 438, 012001.
11. R. Cabrera-Trujillo, S. A. Cruz, *Phys. Rev. A* **2013**, 87, 012502.
12. K. D. Sen (Ed.), *Electronic Structure of Quantum Confined Atoms and Molecules*, Springer, Switzerland **2014**.
13. L. E. Brus, *J. Chem. Phys.* **1984**, 80, 4403.
14. S. Sato, S. Seki, G. F. Luo, M. Suzuki, J. Lu, S. Nagase, T. Akasaka, *J. Am. Chem. Soc.* **2012**, 134, 11681.
15. M. Anaya, A. Rubino, T. C. Rojas, J. F. Galisteo-López, M. E. Calvo, H. Míguez, *Adv. Opt. Mater.* **2017**, 5, 1601087.
16. S. Tarucha, D. G. Austing, T. Honda, R. J. van der Hage, L. P. Kouwnhoven, *Phys. Rev. Lett.* **1996**, 77, 3613.

17. S. Lumb, S. Lumb, V. Prasad, *Phys. Lett. A* **2015**, 379, 1263.
18. E. V. Ludeña, *J. Chem. Phys.* **1978**, 69, 1770.
19. J. Garza, R. Vargas, A. Vela, *Phys. Rev. E* **1998**, 58, 3949.
20. J.-P. Connerade, R. Semaoune, *J. Phys. B* **2000**, 33, 251.
21. N. Aquino, G. Campoy, H. E. Montgomery, Jr, *Int. J. Quantum Chem.* **2007**, 107, 1548.
22. A. Borgoo, D. J. Tozer, D. Geerlings, F. De Proft, *Phys. Chem. Chem. Phys.* **2008**, 10, 1406.
23. A. Sarsa, C. Le Sech, *J. Chem. Theory Comput.* **2011**, 7, 2786.
24. J. Garza, J. M. Hernández-Pérez, J. Z. Ramírez, R. Vargas, *J. Phys. B* **2012**, 45, 015002.
25. J. Gorecki, W. Byers-Brown, *J. Phys. B* **1998**, 21, 403.
26. J. Katriel, H. E. Montgomery, Jr., *J. Chem. Phys.* **2012**, 137, 114109.
27. M. Rodríguez-Bautista, C. Díaz-García, A. M. Navarrete-López, R. Vargas, J. Garza, *J. Chem. Phys.* **2015**, 143, 034103.
28. A. Sarsa, J. M. Alcaraz-Pelegriña, C. Le Sech, *J. Phys. Chem. B* **2015**, 119, 14364.
29. L.G. Jiao, L.R. Zan, Y.Z. Zhang and Y.K. Ho, *Int. J. Quantum Chem.* **2017**, 117, 25375
30. J.-P. Connerade, R. Semaoune, *J. Phys. B* **2000**, 33, 3467.
31. L. D. Landau, E. M. Lifshitz, *Quantum Mechanics. Non Relativistic Theory.* Pergamon Press 1977.
32. C. Couratin *et al.* *Phys. Rev. Lett.* **2012**, 108, 243201.
33. H. A. Bethe, E. W. Sapleter, *Quantum Mechanics of one and two electron atoms.* Springer 1957.
34. A. Holubec, A. D. Stauffer, *J. Phys. A* **1985**, 18, 2141.

35. R. J. W. Hodgson, *J. Phys. A* **1988**, *21*, 679.

36. E. Buendía, F.J. Gálvez, A. Puertas, *J. Phys. A* **1995**, *28*, 6731.

Figure 1: Ionization probability as a function of the confinement radius for states of different shells of the hydrogen atom with the same orbital angular momentum l . The lines are for guiding the eyes. Note that in the plot for $l = 3$ the y range is different from the others.

Figure 2: Ionization probability as a function of the confinement radius for orbitals of the hydrogen atom with the same n and different l values. The lines are for guiding the eyes. Note that in the plot for $n = 4$ the y range is different from the others.

Figure 3: Probability density function of the ionization energy for different states and confinement radii.

Figure 4: Radial $u(r)$ functions for a confined state with $r_c = 2.1167 \text{ \AA}$ as compared with the radial $u(r)$ functions of the ionized electron at different energies and the product of both radial functions that gives the transition probability.

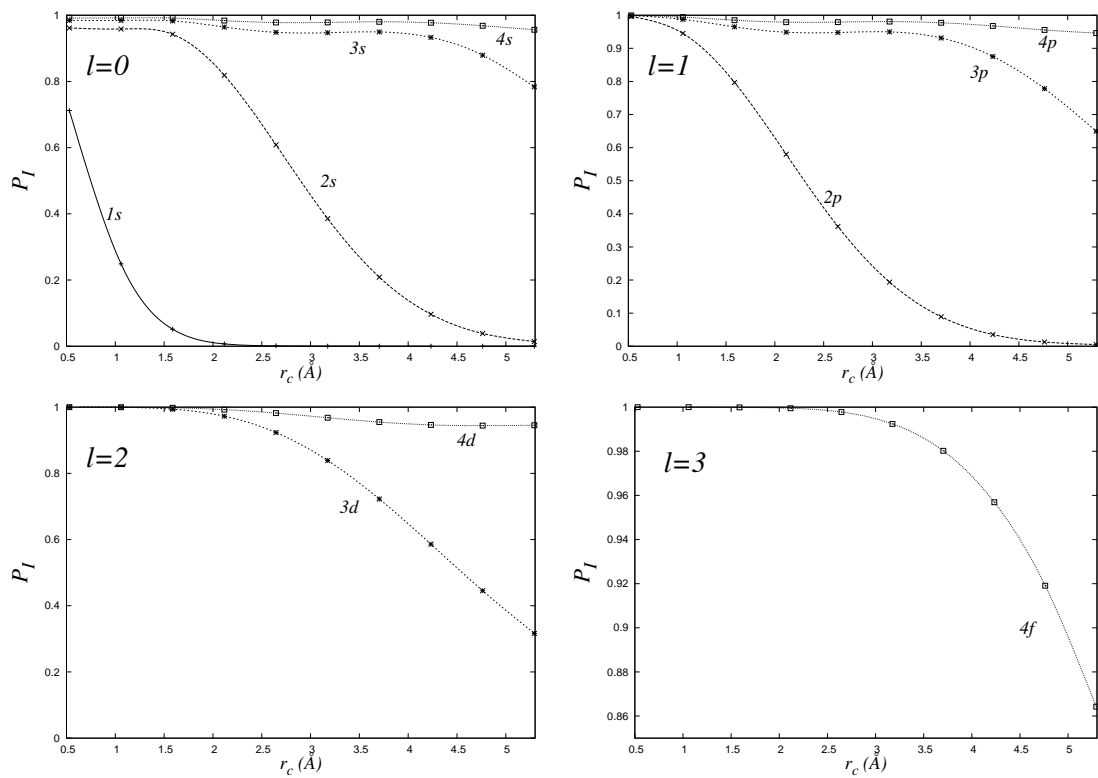


Figure 1
 Morcillo M F, Alcaraz-Pelegrina J M,
 Sarsa A
 Int. J. Quant. Chem.

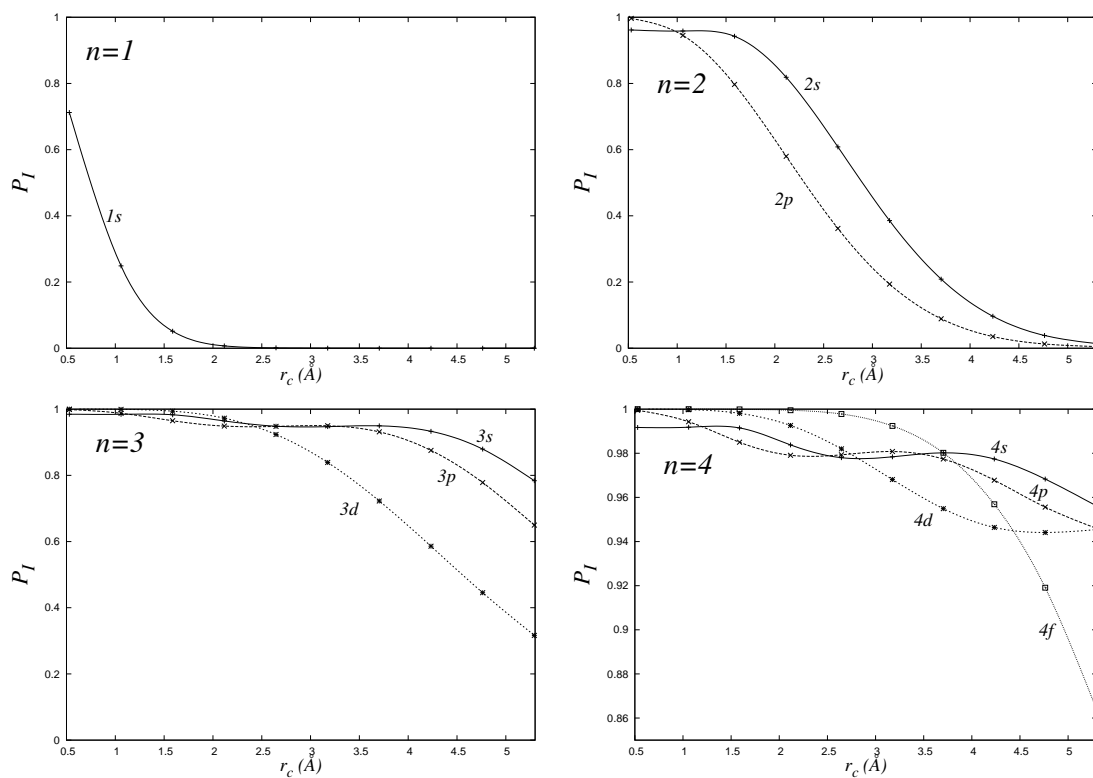


Figure 2
 Morcillo M F, Alcaraz-Pelegrina J M,
 Sarsa A
 Int. J. Quant. Chem.

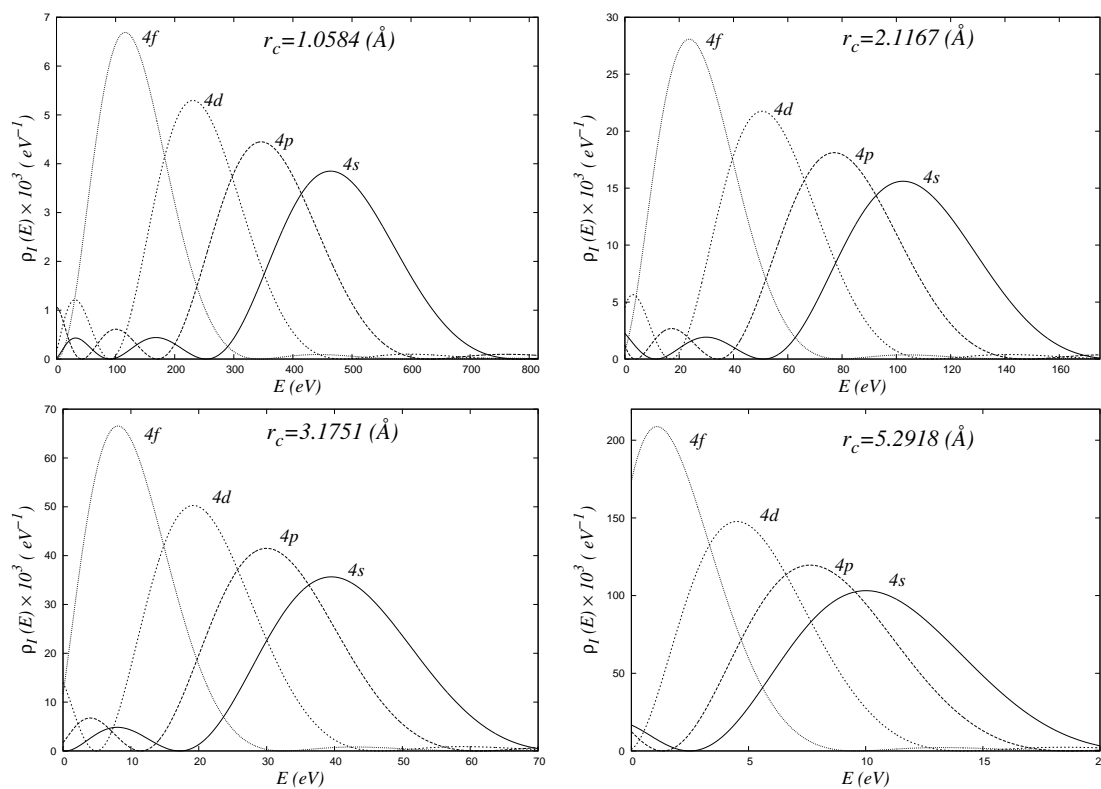


Figure 3
 Morcillo M F, Alcaraz-Pelegrina J M,
 Sarsa A
 Int. J. Quant. Chem.

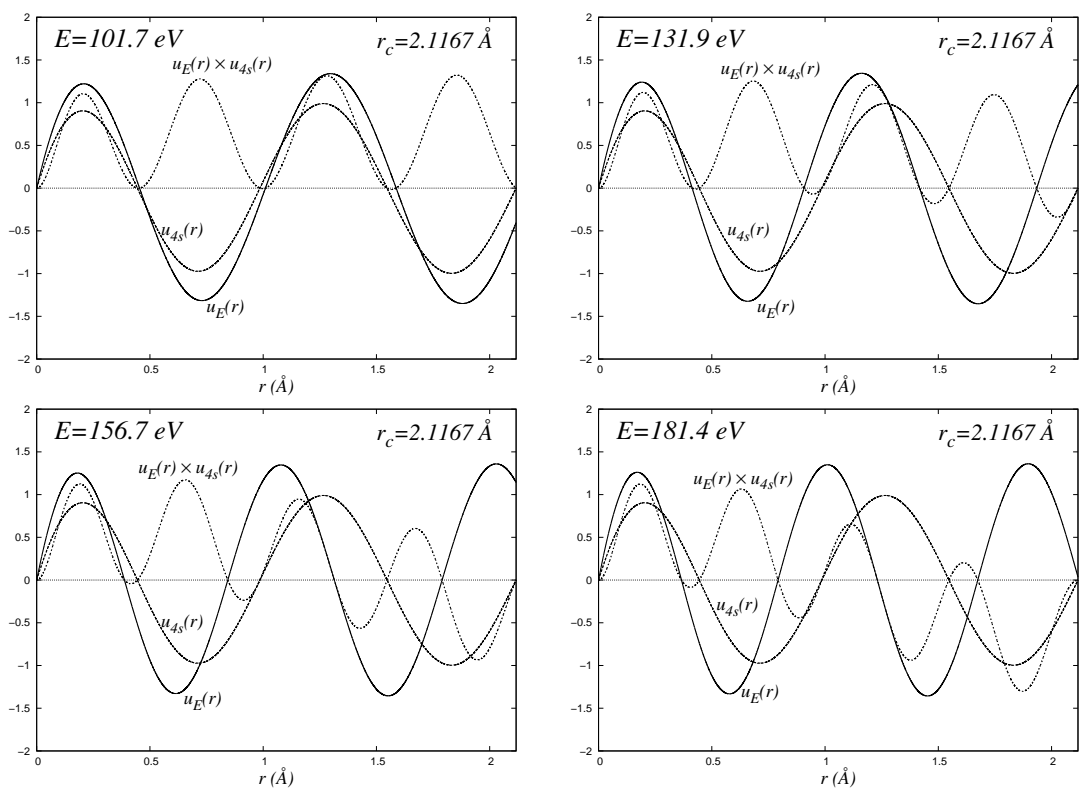


Figure 4
 Morcillo M F, Alcaraz-Pelegrina J M,
 Sarsa A
 Int. J. Quant. Chem.

State	$r_c = 0.5292 \text{ \AA}$		$r_c = 1.0584 \text{ \AA}$	
	E (eV)	P_I	E (eV)	P_I
1s	64.59958187	0.7121	-3.40142325	0.2488
2s	450.89963501	0.9615	90.54613614	0.9584
2p	223.76299102	0.9965	42.88565555	0.9452
3s	1111.94225750	0.9847	253.45094295	0.9844
3p	747.60549169	0.9990	170.58825493	0.9875
3d	407.28544299	1.0000	90.54613614	0.9994
4s	2044.40484855	0.9917	484.80059749	0.9918
4p	1544.46476988	0.9995	367.64172093	0.9943
4d	1069.82434508	1.0000	253.45094295	0.9998
4f	623.02714546	1.0000	145.36579242	1.0000

Table 1: Energy of different initial confined states and ionization probability after leaving confinement for $r_c = 0.5292 \text{ \AA}$ and $r_c = 1.0584 \text{ \AA}$.

	$r_c = 1.5875 \text{ \AA}$		$r_c = 2.1167 \text{ \AA}$	
State	E (eV)	P_I	E (eV)	P_I
<i>1s</i>	-11.53673753	0.0513	-13.15031869	0.0070
<i>2s</i>	30.25048252	0.9425	11.43519399	0.8186
<i>2p</i>	13.09548803	0.7970	3.90557088	0.5798
<i>3s</i>	101.63338925	0.9830	50.95881881	0.9644
<i>3p</i>	68.46953569	0.9649	34.32774075	0.9488
<i>3d</i>	35.17896888	0.9938	16.90795188	0.9727
<i>4s</i>	203.69452294	0.9915	107.93332450	0.9838
<i>4p</i>	155.11550671	0.9850	82.55679544	0.9791
<i>4d</i>	106.37589379	0.9981	56.28471579	0.9926
<i>4f</i>	59.96451570	0.9999	31.10432718	0.9995

Table 2: Energy of different initial confined states and ionization probability after leaving confinement for $r_c = 1.5875 \text{ \AA}$ and $r_c = 2.1167 \text{ \AA}$.

	$r_c = 2.6459 \text{ \AA}$		$r_c = 3.1751 \text{ \AA}$	
State	E (eV)	P_I	E (eV)	P_I
<i>1s</i>	-13.50819479	0.0011	-13.58602697	0.0003
<i>2s</i>	3.84372267	0.6084	0.34626769	0.3856
<i>2p</i>	0.20664110	0.3619	-1.51174367	0.1938
<i>3s</i>	28.65959273	0.9485	17.19045141	0.9472
<i>3p</i>	19.25799901	0.9479	11.46985647	0.9497
<i>3d</i>	8.95573362	0.9234	4.90732910	0.8390
<i>4s</i>	64.82637029	0.9780	42.07872585	0.9784
<i>4p</i>	49.80835659	0.9793	32.47177348	0.9808
<i>4d</i>	33.73262249	0.9820	21.82387604	0.9681
<i>4f</i>	18.21671626	0.9978	11.46985647	0.9924

Table 3: Energy of different initial confined states and ionization probability after leaving confinement for $r_c = 2.6459 \text{ \AA}$ and $r_c = 3.1751 \text{ \AA}$.

	$r_c = 3.7042 \text{ \AA}$		$r_c = 4.2334 \text{ \AA}$	
State	E (eV)	P_I	E (eV)	P_I
<i>1s</i>	-13.60195356	0.0001	-13.60501546	0.0000
<i>2s</i>	-1.39486636	0.2087	-2.30585806	0.0966
<i>2p</i>	-2.38042532	0.0890	-2.84223108	0.0353
<i>3s</i>	10.67342516	0.9496	6.70738834	0.9330
<i>3p</i>	7.01511210	0.9313	4.28220677	0.8754
<i>3d</i>	2.62833800	0.7225	1.25330875	0.5858
<i>4s</i>	28.77200939	0.9802	20.40553168	0.9774
<i>4p</i>	22.29156598	0.9774	15.86219076	0.9678
<i>4d</i>	14.84868394	0.9549	10.45459377	0.9464
<i>4f</i>	7.55402752	0.9802	5.11096675	0.9569

Table 4: Energy of different initial confined states and ionization probability after leaving confinement for $r_c = 3.7042 \text{ \AA}$ and $r_c = 4.2334 \text{ \AA}$.

	$r_c = 4.7626 \text{ \AA}$		$r_c = 5.2918 \text{ \AA}$	
State	E (eV)	P_I	E (eV)	P_I
<i>1s</i>	-13.60557475	0.0000	-13.60567296	0.0000
<i>2s</i>	-2.79827401	0.0386	-3.06961333	0.0141
<i>2p</i>	-3.09467963	0.0128	-3.23433296	0.0052
<i>3s</i>	4.17102344	0.8793	2.48772811	0.7839
<i>3p</i>	2.51900557	0.7782	1.33854878	0.6496
<i>3d</i>	0.38113089	0.4454	-0.19300448	0.3164
<i>4s</i>	14.85740799	0.9683	11.02481168	0.9562
<i>4p</i>	11.57698506	0.9556	8.60032845	0.9460
<i>4d</i>	7.53318936	0.9441	5.50875141	0.9454
<i>4f</i>	3.50325722	0.9191	2.40117598	0.8643

Table 5: Energy of different initial confined states and ionization probability after leaving confinement for $r_c = 4.7626 \text{ \AA}$ and $r_c = 5.2918 \text{ \AA}$.